

Generalized Adaptive Network Coding Aided Successive Relaying for Noncoherent Cooperation

Li Li, Li Wang, and Lajos Hanzo

Abstract—A generalized adaptive network coding (GANC) scheme is conceived for a multi-user, multi-relay scenario, where the multiple users transmit independent information streams to a common destination with the aid of multiple relays. The proposed GANC scheme is developed from adaptive network coded cooperation (ANCC), which aims for a high flexibility in order to: 1) allow arbitrary channel coding schemes to serve as the cross-layer network coding regime; 2) provide any arbitrary trade-off between the throughput and reliability by adjusting the ratio of the source nodes and the cooperating relay nodes. Furthermore, we incorporate the proposed GANC scheme in a novel successive relaying aided network (SRAN) in order to recover the typical 50% half-duplex relaying-induced throughput loss. However, in support of the coherent detection, in addition to carrying out all the relaying functions, the relays have to estimate the Source-to-Relay channels, which imposes a substantial extra energy consumption and bit rate reduction owing to the inclusion of pilots. Hence noncoherent detection is employed for eliminating the power-hungry channel estimation. Finally, we intrinsically amalgamate our GANC scheme with the joint network-channel coding (JNCC) concept into a powerful three-stage concatenated architecture relying on iterative detection, which is specifically designed for the destination node (DN). The proposed scheme is also capable of adapting to rapidly time-varying network topologies, while relying on energy-efficient detection.

Index Terms—Network coding, successive relaying, noncoherent cooperation.

I. INTRODUCTION

THE family of cooperation techniques heralded by van der Meulen in [1] is capable of achieving a beneficial uplink transmit diversity gain by forming a virtual antenna array (VAA) from the distributed single-antenna-aided mobiles, where having a sufficient spatial separation between the transmit antennas for experiencing independent fading is guaranteed. Substantial capacity-related advances were made by Cover and El Gamal in [2] along with the conception of some basic relaying protocols. Laneman *et al.* analysed the decode-and-forward (DF) as well as amplify-and-forward (AF) protocols in [3], which were extensively employed in the contemporary investigations of cooperative networks.

The network coding concepts [4], [5] were originally proposed for approaching the maximum achievable information

flow in a network by invoking simple coding schemes in the intermediate routers. Since the behaviour of the intermediate network coding relays similar to the relay nodes in the DF aided cooperative network, cross-layer network coding techniques were applied to the physical-layer of cooperative schemes in [6]–[10] for the sake of reducing Bit Error Ratio (BER), while enhancing the energy efficiency and/or the bandwidth efficiency. More particularly, the theoretical bound of the bit error probability of network coding was discussed in [11], and the delay optimization problem of the cross-layer network coding technique was analysed in [12].

Then the concept of “matching code-on-graph with network-on-graph” technique was proposed by Bao and Li in [13], where the network topology was transformed to a bipartite graph of low-density-parity-check (LDPC) codes, or LDPC-like codes. This transformation activates an LDPC code to serve as the cross-layer network code (NC), and demonstrates remarkable flexibility in adapting to both network topology changes and to link failures. Similarly, based on [9], [10], Rebelatto *et al.* employed an attractive class of linear block codes as the cross-layer NC in [14], and transformed the problem of maximizing the cooperative diversity order to the design of a linear block code defined over the finite Galois Field $GF(q)$. In more practical approach, Hausl *et al.* devised an energy-efficient joint network-channel coding (JNCC) scheme for network coded cooperation in [15]. Compared to the separate network and Forward Error Correction (FEC) coding scheme employed in [14], a further coding gain can be achieved with the aid of JNCC.

However, all the practical systems proposed in [9], [10], [13]–[15] for implementing network coded cooperation incur a 50% half-duplex relaying-induced throughput loss, since a practical transceiver cannot transmit and receive simultaneously. This simply halves the bandwidth efficiency. As a remedy, the successive relaying aided network (SRAN) concept was advocated in [16], [17], which is capable of almost entirely recovering the 50% throughput loss. Furthermore, it is hard to expect that in addition to the task of relaying, the relays could altruistically afford the complex and power-hungry task of channel estimation in support of coherent detection. Hence, as an attractive design alternative, low-complexity noncoherent detection techniques dispensing with channel estimation are proposed in conjunction with sophisticated soft-input soft-output (SISO) multiple-symbol differential sphere detection (MSDSD) [18].

Against this background, our novel contribution is

- 1) We extend the concept of “matching code-on-graph with network-on-graph” to arbitrary channel coding schemes,

Manuscript received May 18, 2012; revised November 15, 2012 and January 12, 2013. The associate editor coordinating the review of this letter and approving it for publication was H. Dai.

The authors are with the School of ECS, University of Southampton, SO17 1BJ, United Kingdom (e-mail: {l15e08, lh}@ecs.soton.ac.uk).

The financial support of the European Union under the auspices of the Concerto project, as well as that of the RC-UK under the auspices of the India-UK Advanced Technology Centre known as In-ATC and of the European Research Council’s Advanced Fellow grant is gratefully acknowledged.

Digital Object Identifier 10.1109/TCOMM.2013.022713.120339

and conceive the required new signal processing and transmission arrangements in support of this extension. Consequently, a generalized adaptive network coding (GANC) scheme is proposed for multi-user, multi-relay scenarios.

- 2) We intrinsically amalgamate the successive relaying protocol with the GANC philosophy to conceive a new GANC aided SRAN based DS-CDMA system concept. As a result, the typical 50% half-duplex relaying-induced throughput loss is converted to a potential user-load reduction for the CDMA system, since the interference of the relays is avoided by invoking a pair of low-correlation spreading codes.
- 3) Correspondingly, a generalized iterative detection based three-stage transceiver architecture is created for the proposed GANC aided SRAN, which efficiently detects the information bits of different users.

Notation: Boldface characters are used to represent the matrices and vectors. We will frequently represent a physical object in the form of $X_{ij}^l[k]$, where the superscript l and index k are time domain indices, indicating the k^{th} symbol duration of the l^{th} frame. Furthermore, the subscripts i and j represent the network nodes and imply that X is associated with them.

The rest of the paper is organized as follows. The transmission arrangement, the related signal processing, as well as the major advantages of the proposed GANC aided cooperative network are described in Section II. Then, we incorporate the successive relaying protocol into the GANC aided cooperative scheme in Section III. In Section IV, we design our transceiver architecture, while the relevant simulation results are discussed in Section V. Finally, we conclude in Section VI.

The design-steps of the system are as follows:

1. We attempt to establish the basic framework of the proposed GANC aided cooperative network, which is capable of accommodating arbitrary channel coding schemes as our cross-layer NC, while remaining adaptive to both network topology changes and to link failures.
2. We employ the nonbinary linear block (NBLB) coded GANC and recursive systematic convolutional (RSC) coded GANC as two design examples for clarifying the transmission arrangement, the network codeword construction method, the attainable diversity gain, as well as the achievable throughput of our GANC regime.
3. We transplant our advanced GANC regime into a successive relaying aided network for further improving the achievable spectral efficiency.
4. We attempt to design an energy efficient generalized noncoherent iterative detection based transceiver for realizing the proposed GANC aided SRAN.

II. BASIC MODEL OF GANC AIDED COOPERATION

Consider the uplink of a multiuser DS-CDMA system, where a number of actively communicating Mobile Stations (MS) may roam close to the edge of the DS-CDMA cell. In order to improve the communication quality, some of them, labelled as the Source Nodes (SN) in Fig. 1, namely “ s_1, \dots, s_N ” may invoke GANC aided cooperation by relying on the idle users roaming relatively close to the Base Station

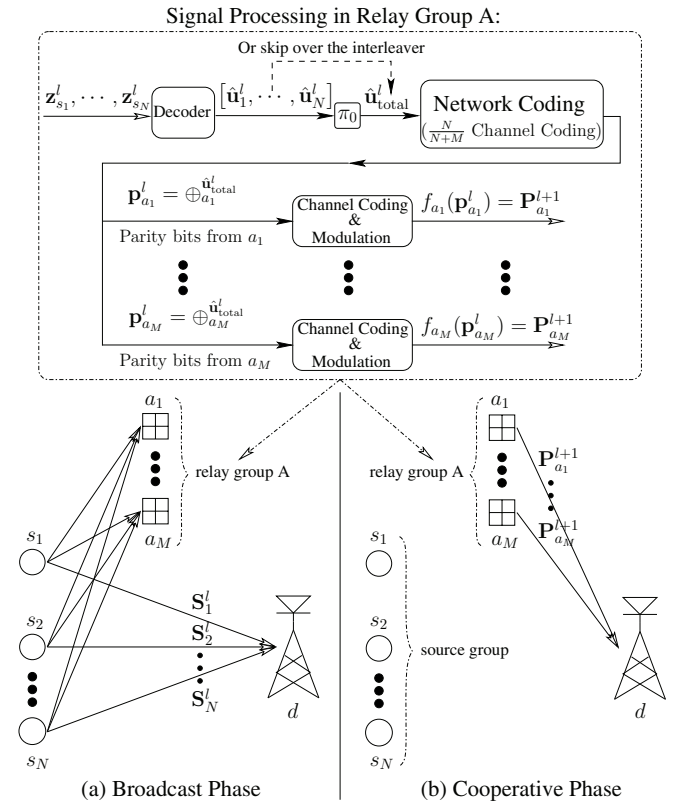


Fig. 1. Basic framework of the proposed GANC aided cooperative network: signal processing and transmission arrangement.

(BS), namely the Destination Node (DN) d as their Relay Nodes (RN). Consequently, a GANC aided cooperative network is created. In the GANC aided cooperative network, the RNs, namely “ a_1, \dots, a_M ” have to negotiate with each other and align their behaviours in support of the GANC scheme. Hence the M RNs actually create a relaying group, which we refer to as “relay group A”.

The path-loss gain achieved by the reduced transmission distance experienced in conventional cooperative systems is also exploited in this contribution. As detailed in [19], when considering the n^{th} SN s_n and m^{th} RN a_m , the average path-loss reductions of the Source-to-Relay (SR) link and Relay-to-Destination (RD) link with respect to the Source-to-Destination (SD) link are given by $G_{s_n a_m} = \left(\frac{D_{s_n d}}{D_{s_n a_m}}\right)^\alpha$ and $G_{a_m d} = \left(\frac{D_{s_n d}}{D_{a_m d}}\right)^\alpha$, respectively, where the notation $D_{ij}, i, j \in \{s_n, a_m, d\}$ represents the distance from node i to node j . Throughout this paper, the path-loss exponent is fixed to $\alpha = 3$ for modelling an urban area. Then we assume that all the channels involved in the GANC aided cooperative network are conventional narrowband time-selective Rayleigh fading channels. In more detail, the fading coefficients $h_{ij}[k], i, j \in \{s_n, a_m, d\}$ of the channel between node i and node j fluctuate according to the associated normalized Doppler frequency f_{ij} . Furthermore, we assume having $(W + N)$ users in the CDMA system, namely the N desired users plus W interfering users.

As detailed in Section I, allowing arbitrary channel coding schemes to serve as the cross-layer NC, while remaining adaptive to both network topology changes and to link failures

is an important advantage of our GANC regime. Hence, as an important design example, the nonbinary linear block (NBLB) codes representing a typical class of channel codes are employed as our cross-layer NC. The resultant nonbinary linear block (NBLB) coded GANC regime is similar to the Diversity Network Coding (DNC) regime of [10] or to the Generalized Distributed Network Coding (GDNC) regime of [14]. Nevertheless, we will demonstrate in the ensuing subsections that compared to the existing regimes of [10], [14], our scheme is capable of achieving the same diversity order, but our solution in terms of adjusting the trade-off between the achievable throughput and the attainable diversity gain has a high flexibility. Moreover, our scheme will additionally benefit from a reduced propagation distance. As another design example, recursive systematic convolutional (RSC) codes invoked as our cross-layer NC are also analysed. We will reveal that the resultant RSC coded GANC regime is also capable of adapting to both network topology changes and to link failures, while striking the same compromise between the achievable throughput and the attainable diversity gain as its nonbinary linear block coded counterpart.

A. Transmission Arrangement

In the proposed GANC aided cooperative network, we segment the source transmissions into identical-length transmission frames of K symbols. This implies that the signal frame \mathbf{S}_n^l transmitted from the n^{th} SN during the l^{th} frame is given by

$$\mathbf{S}_n^l = [S_n^l[1], S_n^l[2], \dots, S_n^l[K]]^T, \quad (1)$$

where $S_n^l[k]$ represents the k^{th} symbol in \mathbf{S}_n^l . The associated information-bit stream carried by \mathbf{S}_n^l is represented by \mathbf{u}_n^l . Specifically, in the NBLB coded GANC regime, we further divide \mathbf{S}_n^l into T_1 identical-length signal blocks in the form of $\mathbf{S}_n^l = [\mathbf{S}_n^l\{1\}, \mathbf{S}_n^l\{2\}, \dots, \mathbf{S}_n^l\{T_1\}]$. The resultant information-bit stream \mathbf{u}_n^l is simultaneously split into T_1 identical-length information-bit packets in the form of $\mathbf{u}_n^l = [\mathbf{u}_n^l\{1\}, \mathbf{u}_n^l\{2\}, \dots, \mathbf{u}_n^l\{T_1\}]$, where an information-bit packet $\mathbf{u}_n^l\{t_1\}$ has b bits. The time required for transmitting a signal block $\mathbf{S}_n^l\{t_1\}$ is treated as a standard time slot, namely T_{Slot} .

The network coding algorithm can be realized with the aid of decoding, re-encoding, as well as re-modulation in the DF based RN. Similar to [9], [10], [13], [14], the proposed GANC aided cooperative network also employs the DF protocol.

Observe during the “(a) Broadcast Phase” of Fig. 1 that, the N SNs $\{s_n\}_{n=1}^N$ simultaneously broadcast N signal frames $\{\mathbf{S}_n^l\}_{n=1}^N$ during the broadcast phase, whose time duration is $T_{\text{Broadcast}}$. Meanwhile, every RN of the relay group A seen in Fig. 1 switches to listening mode in order to receive $\{\mathbf{S}_n^l\}_{n=1}^N$. When ignoring the interference imposed by the interfering users, i.e. assuming $W = 0$, we obtain the k^{th} received signal

of the l^{th} frame at the RN a_m as¹

$$\mathbf{y}_{a_m}^l[k] = \sum_{n=1}^N \sqrt{G_{s_n a_m}} h_{s_n a_m}^l[k] S_n^l[k] \mathbf{C}_{s_n} + \mathbf{n}_{a_m}^l[k], \quad (2)$$

where \mathbf{C}_{s_n} represents the user-specific pseudo-noise (PN) sequence employed by the n^{th} SN s_n of the DS-CDMA system. The spread AWGN vector $\mathbf{n}_{a_m}^l[k]$ obeys $\mathcal{E}\{\mathbf{n}_{a_m}^l[k] \mathbf{n}_{a_m}^{lH}[k]\} = \frac{1}{Q} \sigma^2 \mathbf{I}_Q$, where Q is the spreading factor of \mathbf{C}_{s_n} , while \mathbf{I}_Q is the identity matrix having a dimension of Q . Then the RN a_m decodes $\mathbf{y}_{a_m}^l$, and re-encodes, as well as re-modulates the detected bits according to our specific signal processing scheme, which will be described in Section II-B. Consequently, the signal frame $\mathbf{P}_{a_m}^{l+1}$, which will be forwarded by the RN a_m in the consecutive cooperative phase is prepared. In the same broadcast phase, the k^{th} received signal of the l^{th} frame at the DN d is given by

$$\mathbf{y}_d^l[k] = \sum_{n=1}^N \sqrt{G_{s_n d}} h_{s_n d}^l[k] S_n^l[k] \mathbf{C}_{s_n} + \mathbf{n}_d^l[k]. \quad (3)$$

The overall transmissions during the broadcast phase are overlapped in the same duration of $T_{\text{Broadcast}}$, but separated by different PN sequences.

During the consecutive cooperative phase, whose time duration is $T_{\text{Cooperative}}$, all of the N SNs remain silent. Meanwhile, all of the M RNs of the relay group A switch to their transmission mode, where the signal frames $\{\mathbf{P}_{a_m}^{l+1}\}_{m=1}^M$ are simultaneously forwarded to the DN. The associated k^{th} received signal of the $(l+1)^{\text{st}}$ frame at the DN is given by

$$\mathbf{y}_d^{l+1}[k] = \sum_{m=1}^M \sqrt{G_{a_m d}} h_{a_m d}^{l+1}[k] P_{a_m}^{l+1}[k] \mathbf{C}_{a_m} + \mathbf{n}_d^{l+1}[k], \quad (4)$$

where we have $\mathbf{P}_{a_m}^{l+1} = [P_{a_m}^{l+1}[1], P_{a_m}^{l+1}[2], \dots, P_{a_m}^{l+1}[K]]^T$. The PN sequence \mathbf{C}_{a_m} is employed by the RN a_m to spread its forwarded signals $P_{a_m}^{l+1}[k]$. Similar to the broadcast phase, the overall transmissions during the cooperative phase are overlapped in the same duration of $T_{\text{Cooperative}}$, but separated by the PN sequences assigned to the M idle users in the DS-CDMA uplink, i.e. to the M RNs of relay group A. When employing the NBLB coded GANC regime, we further divide $\mathbf{P}_{a_m}^{l+1}$ into T_2 identical-length signal blocks in the form of $\mathbf{P}_{a_m}^{l+1} = [\mathbf{P}_{a_m}^{l+1}\{1\}, \mathbf{P}_{a_m}^{l+1}\{2\}, \dots, \mathbf{P}_{a_m}^{l+1}\{T_2\}]$. Consequently, the parity-bit stream $\mathbf{p}_{a_m}^{l+1}$ carried by $\mathbf{P}_{a_m}^{l+1}$ is simultaneously split into T_2 identical-length parity-bit packets in the form of $\mathbf{p}_{a_m}^{l+1} = [\mathbf{p}_{a_m}^{l+1}\{1\}, \mathbf{p}_{a_m}^{l+1}\{2\}, \dots, \mathbf{p}_{a_m}^{l+1}\{T_2\}]$, where a parity-bit packet $\mathbf{p}_{a_m}^{l+1}\{t_2\}$ has b bits.

The transmission arrangement during the broadcast phase and that during the cooperative phase will be alternately activated during the consecutive transmission frames. In this contribution, the broadcast phase and cooperative phase always have the same time duration, i.e. we have $T_{\text{Broadcast}} = T_{\text{Cooperative}}; T_1 = T_2$.

¹Since it is difficult to realize perfect synchronization among the users, we assume an asynchronous multiuser CDMA system. By contrast, we assume that perfect synchronization is achieved within the GANC aided cooperative network based on the fact that the total number of its component nodes will remain relatively small.

B. Signal Processing at the Relay Group A

Observe at the top block of Fig. 1 that specifically designed signal processing is implemented at the relay group A in order to realize the GANC scheme. When considering a single RN a_m , relying on the DS-CDMA principle [20], after applying the chip-waveform matched-filter to the waveform of \mathbf{C}_{s_n} , the received signal $\mathbf{y}_{a_m}^l[k]$ of (2) is despread to yield

$$z_{s_n}^l[k] = \sqrt{G_{s_n a_m}} h_{s_n a_m}^l[k] S_n^l[k] + I_{s_{\text{part } a_m}}^l[k] + n_{a_m}^l[k], \quad (5)$$

where the signal component contributed by the n^{th} SN s_n is retained, while the multiple access interference (MAI) $I_{s_{\text{part } a_m}}^l[k]$ imposed by the other $(N-1)$ SNs is suppressed, which is formulated as

$$I_{s_{\text{part } a_m}}^l[k] = \sum_{i=1, \neq n}^N \sqrt{G_{s_i a_m}} h_{s_i a_m}^l[k] S_i^l[k] \gamma_{s_i s_n}, \quad (6)$$

where $\gamma_{s_i s_n}$ represents the cross-correlation (CCL) between \mathbf{C}_{s_i} and \mathbf{C}_{s_n} . Consequently, multiple despread signal frames $\{\mathbf{z}_{s_n}^l\}_{n=1}^N$ are generated at the RN a_m , where we have $\mathbf{z}_{s_n}^l = [z_{s_n}^l[1], z_{s_n}^l[2], \dots, z_{s_n}^l[K]]^T$.

After forwarding the despread signal frame $\mathbf{z}_{s_n}^l$ to the decoder of a_m , the estimate $\hat{\mathbf{u}}_n^l$ of the original information-bit stream \mathbf{u}_n^l is generated. Specifically, when employing the RSC code as our cross-layer NC, the RN activated should be capable of perfectly detecting all the SN's information-bit streams $\{\mathbf{u}_n^l\}_{n=1}^N$, which is a necessary requirement of the RSC coded GANC. For satisfying this requirement, we have to appropriately construct the source group and relay group A. Let \mathcal{R} denote the entire RN resource pool, which consists of the idle users roaming between the SNs and DN. The specific RNs, which perfectly decoded the information-bit stream \mathbf{u}_n^l transmitted by the SN s_n , are selected from \mathcal{R} for the sake of constructing the subset \mathcal{R}_{s_n} . Consequently, when the source group is constituted by $\{s_n\}_{n=1}^N$, where the maximum relay group set in the RSC coded GANC is given by $\{\mathcal{R}_{s_1} \cap \mathcal{R}_{s_2} \cap \dots \cap \mathcal{R}_{s_N}\}$, which implies that we should set "relay group A $\subseteq \{\mathcal{R}_{s_1} \cap \mathcal{R}_{s_2} \cap \dots \cap \mathcal{R}_{s_N}\}$ ".

During the network coding stage, the N SNs create a source group, while the M RNs form the relay group A. Inspired by the "matching code-on-graph with network-on-graph" concept of [13], our basic regime conceived for the proposed GANC consists of three steps:

- (1) **Assign the ratio of the source group size² and the relay group size to the coding rate R_{code} of the cross-layer NC, which is formulated as**

$$R_{\text{code}} = \frac{N}{N+M}. \quad (7)$$

- (2) **Specify the generator matrix of the cross-layer NC.**
- (3) **Distribute the parity bits $\mathbf{p}_{\text{total}}^l$ generated by the GANC scheme among the M RNs.**

When employing the NBLB codes as our cross-layer NC, we consecutively concatenate each estimated information-bit packet $\hat{\mathbf{u}}_n^l$ for the sake of constructing the entire input of the cross-layer NC encoder - $\hat{\mathbf{u}}_{\text{total}}^l$. This process is represented

by the dashed arrow at the top of Fig. 1. Hence we have $\hat{\mathbf{u}}_{\text{total}}^l = [\hat{\mathbf{u}}_1^l, \hat{\mathbf{u}}_2^l, \dots, \hat{\mathbf{u}}_N^l]$. For the NBLB coded GANC, the basic signal processing framework of relay group A depicted at the top of Fig. 1 is further detailed in Fig. 2, which may be formulated as

$$[\mathbf{u}_{\text{total}}^l, \mathbf{p}_{\text{total}}^l] = \hat{\mathbf{u}}_{\text{total}}^l \cdot \mathbf{G}, \quad (8)$$

where $\mathbf{G} = [\alpha \mid \beta]$ is the systematic generator matrix of a nonbinary linear block code, which serves as our cross-layer NC. The specific part of \mathbf{G} , which is denoted by α is an NT_1 -dimensional identity matrix. Then we have $\beta \in \mathbb{C}^{NT_1 \times MT_2}$. Since the entire input $\hat{\mathbf{u}}_{\text{total}}^l$ in (8) consists of NT_1 information-bit packets and because we have $T_1 = T_2$, the dimension of \mathbf{G} is in line with the cross-layer coding rate given in (7).

Observe in Fig. 2 that a parity-bit packet $\mathbf{p}_{a_m}^l\{t_2\}$, which is generated by RN a_m during the broadcast phase, is given by

$$\mathbf{p}_{a_m}^l\{t_2\} = \sum_{n=1}^N \sum_{t_1=1}^{T_1} \beta_{m,t_2}^{n,t_1} \hat{\mathbf{u}}_n^l\{t_1\}, \quad (9)$$

which will be forwarded to DN d in the t_2^{th} time slot during the consecutive cooperative phase. For the sake of adapting to link failures, if we have $\hat{\mathbf{u}}_n^l\{t_1\} \neq \mathbf{u}_n^l\{t_1\}$ in the RN a_m , the corresponding coding coefficients $\{\beta_{m,t_2}^{n,t_1}\}_{t_2=1}^{T_2}$ in Fig. 2 are fixed to zero value. Hence all the parity-bit packets $\{\mathbf{p}_{a_m}^l\{t_2\}\}_{t_2=1}^{T_2}$ generated at the RN a_m are irrelevant to $\hat{\mathbf{u}}_n^l\{t_1\}$, because we discard this corrupted data. Let \mathcal{D}_{n,t_1} denote the specific set of RNs, which succeed in correctly decoding $\mathbf{u}_n^l\{t_1\}$ during the broadcast phase. Correspondingly, the number of RNs contained in the set \mathcal{D}_{n,t_1} is denoted by $|\mathcal{D}_{n,t_1}|$. Let $\mathcal{D}_{n,t_1}(I)$ denote the set of all information-bit packets correctly decoded by the RNs in the set \mathcal{D}_{n,t_1} during the broadcast phase, including $\mathbf{u}_n^l\{t_1\}$ itself. Similarly, the number of information-bit packets contained in the set $\mathcal{D}_{n,t_1}(I)$ is denoted by $|\mathcal{D}_{n,t_1}(I)|$. According to [5], [10], the generator matrix \mathbf{G} seen in Fig. 2 should allow us to recover the entire information-bit packet set $\mathcal{D}_{n,t_1}(I)$ from any correctly decoded $|\mathcal{D}_{n,t_1}(I)|$ packets³ at the DN for the sake of maximizing the diversity order of the NBLB coded GANC. The generator matrix construction method introduced in [14] satisfies this requirement, hence it may be employed for specifying the coefficients β_{m,t_2}^{n,t_1} in (9).

Observe at the DN that, the systematic part of the whole network codeword, i.e. the $\mathbf{u}_{\text{total}}^l$ part of $[\mathbf{u}_{\text{total}}^l, \mathbf{p}_{\text{total}}^l]$, is gleaned from the Source-to-Destination transmissions during the broadcast phase, while, the remaining parity part $\mathbf{p}_{\text{total}}^l = [\mathbf{p}_{a_1}^l, \mathbf{p}_{a_2}^l, \dots, \mathbf{p}_{a_M}^l]$ is gleaned from the Relay-to-Destination transmissions during the cooperative phase. Hence the DN may first individually decode every $\mathbf{u}_n^l\{t_1\}$ and $\mathbf{p}_{a_m}^l\{t_2\}$ vectors, and then jointly decodes $\{\{\mathbf{u}_n^l\{t_1\}\}_{t_1=1}^{T_1}\}_{n=1}^N$ based on the structure of the cross-layer NC illustrated in Fig. 2.

Then, in the RSC coded GANC, we generate $\hat{\mathbf{u}}_n^l = \mathbf{u}_n^l, n \in \{1, 2, \dots, N\}$ at every RN as a benefit of our relay group selection strategy introduced at the beginning of this subsection. Similar to the NBLB coded GANC, at the RN we concatenate

²The size of the source group is given by the number of SNs included in the source group. A similar definition is stipulated for the relay group size.

³This $|\mathcal{D}_{n,t_1}(I)|$ packets should belong to the packet set, which is related to the information-bit packet set $\mathcal{D}_{n,t_1}(I)$ and consists of $|\mathcal{D}_{n,t_1}(I)| + |\mathcal{D}_{n,t_1}|T_2$ packets received at the DN d .

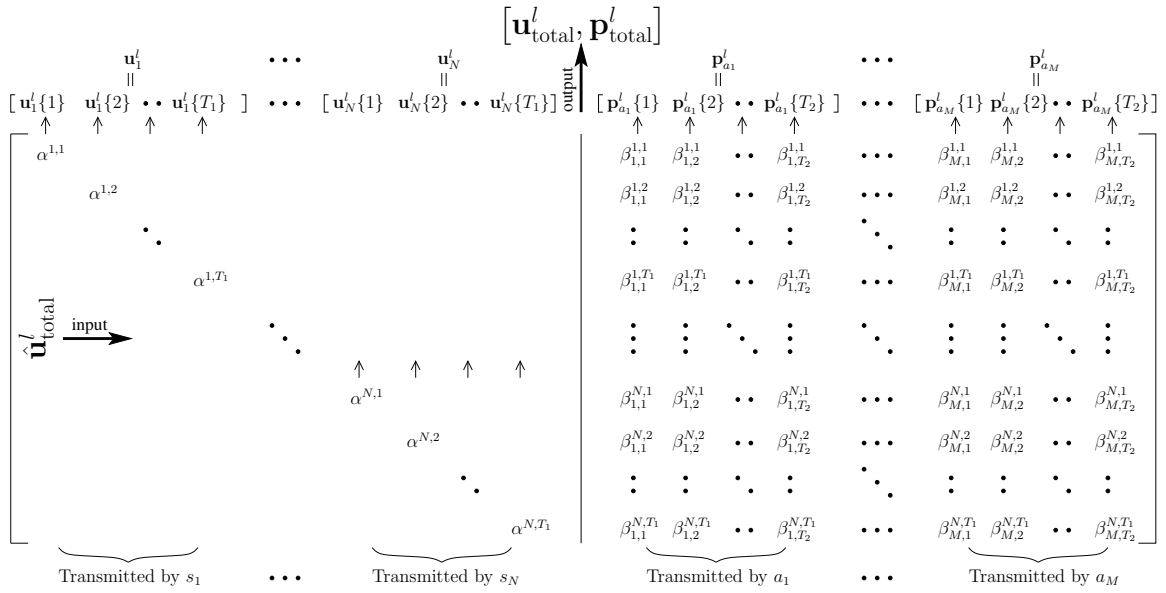


Fig. 2. Illustration of the systematic generator matrix and the network coding process engaged in the NBLB coded GANC.

every detected \mathbf{u}_n^l for creating a single information-bit stream in the form of $[\mathbf{u}_1^l, \mathbf{u}_2^l, \dots, \mathbf{u}_N^l]$. However, for the sake of eliminating the ensuing fading-induced correlation among the symbols of the signal frames \mathbf{S}_n^l and \mathbf{P}^{l+1} , the combined detected information-bit stream $[\mathbf{u}_1^l, \mathbf{u}_2^l, \dots, \mathbf{u}_N^l]$ is further interleaved. This operation is represented by the notation “ π_0 ” in Fig. 1. Hence the entire input of the cross-layer NC becomes $\mathbf{u}_{\text{total}}^l = \text{Interleaver}([\mathbf{u}_1^l, \mathbf{u}_2^l, \dots, \mathbf{u}_N^l])$, which consists of NT_1b bits. According to the first step of the proposed basic GANC regime, a $(\frac{N}{N+M})$ -rate RSC code is employed at the RN as the cross-layer NC. Naturally, its generator polynomials should aim for maximizing the RSC code’s free distance d_{free} , because maximizing the free distance of the $(\frac{N}{N+M})$ -rate RSC code is equivalent to maximizing the diversity order of the associated GANC aided cooperative network, which will be revealed in Section II-C.

After fixing the cross-layer NC, the overall signal processing carried out in relay group A for the RSC coded GANC is further detailed in Fig. 3. The resultant network codeword \mathbf{c} may be formulated as

$$\mathbf{c} = [\mathbf{u}_{\text{total}}^l, \mathbf{p}_{\text{total}}^l] = \mathbf{u}_{\text{total}}^l \cdot \mathbf{G} = \mathbf{u}_{\text{total}}^l \cdot [\mathbf{I} \mid \mathbf{P}], \quad (10)$$

where \mathbf{G} is the systematic generator matrix of the $(\frac{N}{N+M})$ -rate RSC code, while \mathbf{I} is an NT_1b -dimensional identity matrix, and $\mathbf{P} \in \mathbb{C}^{NT_1b \times MT_2b}$. Since $\mathbf{u}_{\text{total}}^l$ consists of NT_1b bits, according to the coding rate of $(\frac{N}{N+M})$ and bearing in mind that we have $T_1 = T_2$, $\mathbf{p}_{\text{total}}^l$ will consist of MT_2b bits, which is further split into M parity-bit streams $\{\mathbf{p}_{a_m}^l\}_{m=1}^M$, where every parity-bit stream $\mathbf{p}_{a_m}^l$ consists of T_2b bits.

The network encoding process represented by (10) and the ensuing partitioning of $\mathbf{p}_{\text{total}}^l$, i.e. we consecutively split $\mathbf{p}_{\text{total}}^l$ into M parity-bit streams $\{\mathbf{p}_{a_m}^l\}_{m=1}^M$, are implemented at every RN of relay group A. Hence we obtain $\mathbf{p}_{\text{total}}^l = [\mathbf{p}_{a_1}^l, \mathbf{p}_{a_2}^l, \dots, \mathbf{p}_{a_M}^l]$ at every RN. According to the third step of the proposed basic GANC regime outlined in this section,

the RN a_1 may be only responsible for the transmission of the parity-bit stream $\mathbf{p}_{a_1}^l$. Hence $\mathbf{p}_{a_1}^l$ is extracted from $\mathbf{p}_{\text{total}}^l$, and re-encoded, as well as re-modulated for creating the signal frame $\mathbf{P}_{a_1}^{l+1}$ at the RN a_1 , which will be further forwarded from the RN a_1 to the DN d during the cooperative phase. Similar operations will be carried out in all the other RNs $a_m, m = 2, 3, \dots, M$. This allocation of the parity part of the network codeword \mathbf{c} is also illustrated at the lower right corner of Fig. 3.

C. Advantages of GANC Aided Cooperation

For the NBLB coded GANC, the achievable diversity order is given by⁴

$$D_{\text{GANC}} = (M - |\mathcal{D}_{n,t_1}|) + |\mathcal{D}_{n,t_1}|T_2 + 1, \quad (11)$$

where we have $|\mathcal{D}_{n,t_1}| \in [0, M]$. Hence the range of D_{GANC} is given by

$$M + 1 \leq D_{\text{GANC}} \leq MT_2 + 1. \quad (12)$$

According to (11), the diversity order of the proposed NBLB coded GANC is almost the same as that of the DNC regime proposed in [10] or that of the GDNC scheme proposed in [14]. The only difference is that the minimum value of $|\mathcal{D}_{n,t_1}|$ equals to 1 in the DNC or GDNC regime, since the SN continues to serve as the RN in [10], [14], whilst, it drops to 0 in our system, since we employ other idle users as our RNs.

Let us now analyse the diversity order of the RSC coded GANC. Let $\{\mathbf{c}_1, \mathbf{c}_2, \dots, \mathbf{c}_M\}$ represent the set of all the legitimate network codewords generated from (10). Since the input information-bit stream $\mathbf{u}_{\text{total}}^l$ of the RSC code exploited

⁴According to the similarity, the diversity derivation of the generalized dynamic-network codes (GDNC) exhibited in [14] can be straightforwardly applied to here. For the space economy, we omit the detailed derivation of (11) and refer to [14, Section V] for further information.

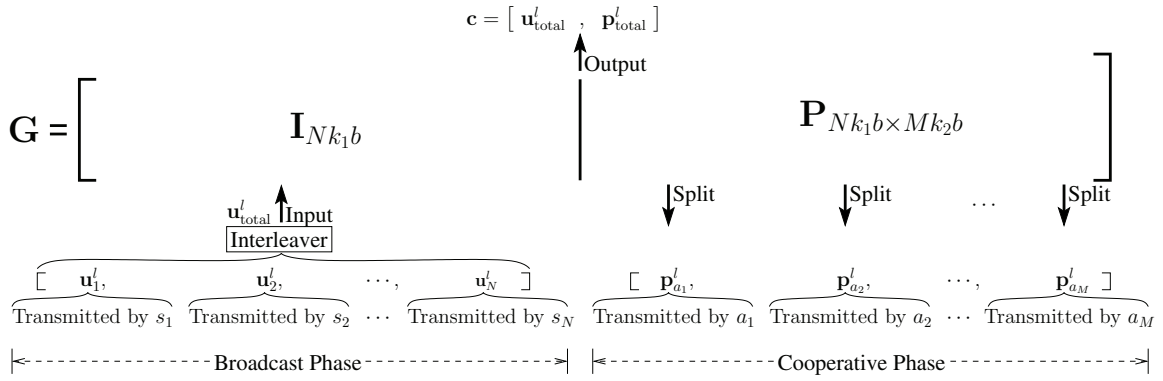


Fig. 3. Illustration of the network coding process engaged in the RSC coded GANC.

in (10) has NT_1b bits, the total number of all the legitimate network codewords is $\mathcal{M} = 2^{NT_1b}$. Then, let $\mathbf{c}_i(k)$ denote the k^{th} bit of network codeword \mathbf{c}_i , where we have $k \in \{1, 2, \dots, NT_1b + MT_2b\}$. According to [21, Chapter 3], when experiencing an i.i.d $\mathcal{CN}(0, 1)$ Rayleigh fading channel, the upper bound of the overall probability of erroneously decoding the network codeword \mathbf{c} in (10) is given by

$$P_{\text{outage}} \leq \frac{4^{d_{\text{free}}}}{\mathcal{M}} \sum_{i \neq j} \frac{1}{\delta_{ij}} \text{SNR}^{-d_{\text{free}}} \leq \frac{4^{d_{\text{free}}} (\mathcal{M} - 1)}{\min_{i \neq j} \delta_{ij}} \text{SNR}^{-d_{\text{free}}}, \quad (13)$$

where δ_{ij} is the squared product distance between \mathbf{c}_i and \mathbf{c}_j , which is evaluated as

$$\delta_{ij} = \prod_{k=1}^{NT_1b + MT_2b} |\mathbf{c}_i(k) - \mathbf{c}_j(k)|^2. \quad (14)$$

As stated in [22] and in [23, Section III], the free distance of a systematic convolutional code is upper bounded by the minimum distance of the associated best linear block code. When considering the Singleton bound [24, Chapter 7], the achievable free distance d_{free} is given by

$$d_{\text{free}} = (NT_1b + MT_2b) - (NT_1b) + 1 = MT_2b + 1. \quad (15)$$

In order to represent the upper bound of P_{outage} in a block-based form, after substituting (15) into (13), we arrive at

$$\begin{aligned} P_{\text{outage}} &\leq \frac{4^{2(MT_2b+1)} (\mathcal{M} - 1)}{\min_{i \neq j} \delta_{ij}} \left[\left(\frac{1}{4\text{SNR}} \right)^b \right]^{MT_2 + \frac{1}{b}} \\ &\leq \frac{4^{2(MT_2b+1)} (\mathcal{M} - 1)}{\min_{i \neq j} \delta_{ij}} (P_e)^{MT_2 + \frac{1}{b}}, \end{aligned} \quad (16)$$

where P_e is the outage probability of a signal block (i.e. of an information-bit packet), which has the same definition as that given in [10, (2)]. Based on (16), the block based diversity order of our RSC coded GANC is given by

$$D_{\text{GANC}} = MT_2 + \frac{1}{b} \approx MT_2 + 1. \quad (17)$$

Hence, observe from (12) that, if perfect detection is achieved at every RN pertaining to the relay group A⁵, the RSC coded GANC becomes capable of achieving the same diversity order

⁵For the NBLB coded GANC, it means that $|\mathcal{D}_{n,t_1}|$ in (11) equals to M .

as the NBLB coded GANC, or the DNC of [10], or the GDNC of [14].

Then, the average throughput of the whole system may be quantified by the ratio of the total number of transmitted information bits divided by the number of orthogonal time slots and codes required, which is similar to the concept of the overall rate defined in [14, (14)]. In line with [10], [13], [14], we also assume that every node in our GANC aided cooperative network transmits its messages at the same rate of X bits/s. Therefore, according to the transmission arrangement illustrated in Fig. 1 and bearing in mind that we have $T_{\text{Broadcast}} = T_{\text{Cooperative}}$, the average throughput of our GANC aided cooperative network is given by

$$\mathcal{T}_{\text{ave}} = \frac{\overbrace{N \cdot T_{\text{Broadcast}} \cdot X}^{\text{Transmitted information}}}{\underbrace{N \cdot T_{\text{Broadcast}} + M \cdot T_{\text{Cooperative}}}_{\text{Consumed orthogonal channels}}} = \frac{N}{N + M} \cdot X \quad \text{bits/s}. \quad (18)$$

Recall that in the ANCC regime of [13], the throughput \mathcal{T}_{ave} is inherently constrained to $\frac{1}{2}$, since each SN will also serve as a RN during the cooperative phase, while in the DNC regime of [10] and GDNC regime of [14] different \mathcal{T}_{ave} values can be achieved by varying the broadcast phase to cooperative phase duration. By contrast, based on (12), (17), and (18), our GANC aided cooperative network is capable of striking an arbitrary trade-off between the attainable diversity gain and the achievable throughput by appropriately adjusting the relay group size (or source group size). Since there may be an abundant supply of RN candidates constituted by the idle mobile users in the DS-CDMA uplink for constructing the relay group A, it is entirely unproblematic to allow nodes to join or disjoin the source group or the relay group A. Hence the technique of adjusting the diversity order and/or throughput facilitated by our GANC regime exhibits a high flexibility.

Furthermore, since the RNs relied upon in our GANC regime are selected from the set of idle users of the DS-CDMA system, we may argue that the user-specific PN sequence \mathbf{C}_{a_m} assigned to the RN a_m may be readily exploited by our GANC aided cooperative network. Hence we may argue that the GANC aided cooperative network only requires $T_{\text{Cooperative}}$ orthogonal time slots during the cooperative phase.

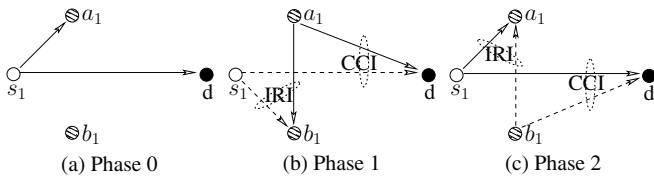


Fig. 4. The framework of a typical SRAN.

Consequently, the average throughput \mathcal{T}_{ave} in (18) becomes

$$\mathcal{T}_{ave} = \frac{N \cdot T_{Broadcast} \cdot X}{N \cdot T_{Broadcast} + T_{Cooperative}} = \frac{N}{N+1} \cdot X \quad \text{bits/s.} \quad (19)$$

As a result, the previously mentioned trade-off between the attainable diversity gain and achievable throughput may also be interpreted as a trade-off between the achievable transmission integrity of our GANC aided cooperative network and the potential user-load reduction of the DS-CDMA system.

Based on the analysis of the two typical applications of the proposed GANC regime employing NBLB codes and RSC codes as the cross-layer NC, respectively, it may be concluded that for a moderate network size, where the RNs are capable of affording a relatively high detection complexity, the RSC coded GANC scheme is preferred. By contrast, the NBLB coded GANC scheme will be preferred for large networks, especially when the RNs have different error correction capability. In more depth, it also reveals that the basic framework of our GANC aided cooperative network depicted in Fig. 1 is capable of accommodating arbitrary channel coding schemes as our cross-layer NC, while retaining its adaptivity to both network topology changes and to link failures. Alternatively, the solutions of [13] and [14] may be treated as two specific realizations of our proposed GANC algorithm. Compared to the existing advanced network coding schemes of [10], [13], [14], our GANC aided cooperative network achieves a beneficial trade-off between the attainable diversity gain and the achievable throughput. Furthermore, our GANC aided cooperative network further benefits from the path-loss reduction achieved in the Source-to-Relay and Relay-to-Destination links, which will be demonstrated in Section V.

III. INCORPORATION OF SUCCESSIVE RELAYING

As stated in Section II-C, although the PN sequence C_{a_m} may be readily available for relaying, the proposed GANC aided regime still incurs a relative throughput loss of at least $\frac{1}{N+1}$, as the result of obeying the basic half-duplex three-terminal cooperative network arrangement. Hence, in order to recover the throughput loss, we amalgamated the successive relaying regime proposed in [16], [17] with our GANC aided cooperative scheme.

The DF based SRAN regime is portrayed in Fig. 4, where the SN s_1 employs two relays, namely a_1 and b_1 to alternately assist its Up Link (UL) transmissions. In more detail, in Phase 0 of Fig. 4, s_1 broadcasts its information stream, while a_1 listens to s_1 and b_1 remains silent. Then, in Phase 1 of Fig. 4, s_1 continues to broadcast its next information stream, while a_1 decodes, re-encodes and forwards the signals received from s_1

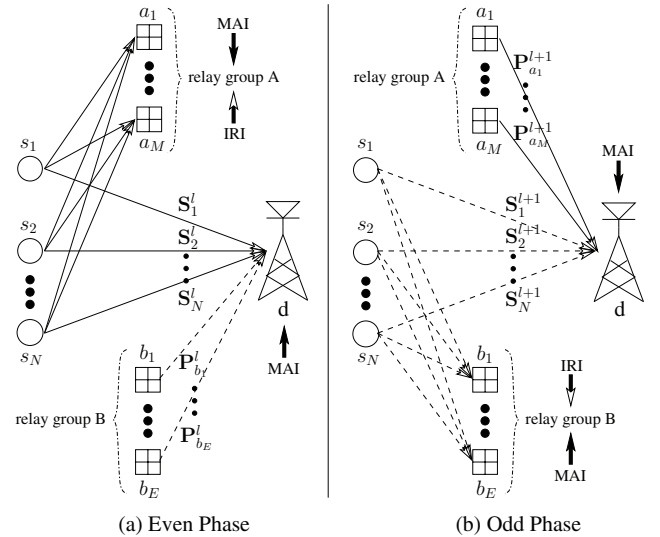


Fig. 5. Schematic of the GANC aided SRAN.

during Phase 0 and b_1 listens to s_1 . By contrast, in Phase 2 of Fig. 4, s_1 broadcasts its third information stream, but the roles of a_1 and b_1 are reversed. In the future phases, the transmission scheduling of Phase 1 and 2 portrayed in Fig. 4 are repeated. A critical problem of the SRAN is the successive relaying-induced inferences generated both at the RN and at the DN [16], [25], namely the inter-relay interference (IRI) and the co-channel interference (CCI), respectively. Observe in Fig. 4 that the IRI arises due to the fact that the signal forwarded by one of the two RNs will contaminate the reception of the signal broadcast by the SN at the other RN. By contrast, the CCI arises due to the fact that the signal forwarded by the RN and that broadcast by SN may simultaneously arrive at the DN, where these signals will interfere with each other.

By adding another relay group, namely “relay group B” to the basic model of our GANC aided cooperation portrayed in Fig. 1, as well as simultaneously replacing the previous transmission arrangement described in Section II-A by the successive relaying regime, we arrive at the GANC aided SRAN seen in Fig. 5⁶.

Observe in Fig. 5 that the relay group B consists of E RNs, namely “ b_1, \dots, b_E ”, which also uses the same signal processing as that detailed in Section II-B for relay group A. Consequently, when relay group B listens to the source group during the odd phase of Fig. 5, each RN b_e generates its transmission frame $\mathbf{P}_{b_e}^l = [P_{b_e}^l[1], \dots, P_{b_e}^l[K]]^T$, which carries the parity-bit stream $\mathbf{p}_{b_e}^l$. Then, the RN b_e forwards the signal frame $\mathbf{P}_{b_e}^l$ to the DN during the even phase. Similar to [16], [17], we assume that the GANC aided SRAN constituted by the source group, the relay groups A and B, as well as

⁶The transmission arrangements of the first and last phases in the SRAN are different from the other phases, as also seen in [26, Fig.1]. Nevertheless, when the total number of transmission phases in the SRAN is sufficiently high, we may use the transmission arrangements of two typical phases, e.g. Phases 1 and 2 of Fig. 4 to summarize the entire transmission arrangement of the SRAN, where the slight inaccuracies incurred during the first and last phases are ignored. Similarly, the holistic transmission arrangement of the GANC aided SRAN is summarized in the form of two typical phases, namely the “Even Phase” and “Odd Phase” in Fig. 5.

the common DN d portrayed in Fig. 5 are perfectly aligned in the time-domain by forming a synchronous system. Hence the k^{th} signal of the l^{th} frame received at the DN during the even phase of the GANC aided SRAN is given by

$$\mathbf{y}_d^l[k] = \sum_{n=1}^N \sqrt{G_{s_n d}} h_{s_n d}^l[k] S_n^l[k] \mathbf{C}_{s_n} + \sum_{e=1}^E \sqrt{G_{b_e d}} h_{b_e d}^l[k] P_{b_e}^l[k] \mathbf{C}_{b_e} + \sum_{w=1}^W \sqrt{G_{s_w d}} h_{s_w d}^l[k] S_w^l[k] \mathbf{C}_{s_w} + \mathbf{n}_d^l[k], \quad (20)$$

where we have $l = 0, 2, 4, \dots$. Then the k^{th} signal of the $(l+1)^{st}$ frame received at the DN in the consecutive odd phase of the GANC aided SRAN is given by

$$\mathbf{y}_d^{l+1}[k] = \sum_{n=1}^N \sqrt{G_{s_n d}} h_{s_n d}^{l+1}[k] S_n^{l+1}[k] \mathbf{C}_{s_n} + \sum_{m=1}^M \sqrt{G_{a_m d}} h_{a_m d}^{l+1}[k] P_{a_m}^{l+1}[k] \mathbf{C}_{a_m} + \sum_{w=1}^W \sqrt{G_{s_w d}} h_{s_w d}^{l+1}[k] S_w^{l+1}[k] \mathbf{C}_{s_w} + \mathbf{n}_d^{l+1}[k]. \quad (21)$$

According to the signal processing stipulated in Section II-B and to the transmission arrangement of the GANC aided SRAN portrayed in Fig. 5, the N signal frames $\{\mathbf{S}_n^l\}_{n=1}^N$ broadcast by the source group in the l^{th} frame (the even phase of Fig. 5) and the M signal frames $\{P_{a_m}^{l+1}\}_{m=1}^M$ forwarded by the relay group A in the $(l+1)^{st}$ frame (the odd phase of Fig. 5) correspond to the information part and parity-bit part of the cross-layer NC output in the relay group A, respectively. Hence the receiver at the DN should collect these two types of signal frames in order to jointly detect the original information-bit streams $\{\mathbf{u}_n^l\}_{n=1}^N$. However, according to (20), the information-bearing symbols $\{S_n^l[k]\}_{n=1}^N$ contaminate each other and are further contaminated by the other signal components of $\mathbf{y}_d^l[k]$, which impose CCI and MAI. The symbols $\{P_{a_m}^{l+1}[k]\}_{m=1}^M$ in (21) incur a similar interference problem. Fortunately, as a benefit of operating our GANC aided SRAN in the context of a DS-CDMA system, we may exploit the DS-CDMA philosophy to retain the desired component in $\mathbf{y}_d^l[k]$ (or $\mathbf{y}_d^{l+1}[k]$), while suppressing the interference components.

Similar to the operations involved in (5), when the chip-waveform matched-filter of the DN is matched to the waveform of \mathbf{C}_{s_n} , the symbol $S_n^l[k]$ directly transmitted by the SN s_n will contribute the main component of the despread signal $\mathbf{y}_d^l[k]$, while the other components of (20) - including all the other information bearing symbols $\{S_i^l[k]\}_{i=1, \neq n}^N$ - become the interference components. The associated output of the chip-waveform matched-filter is given by

$$z_{s_n}^l[k] = \sqrt{G_{s_n d}} h_{s_n d}^l[k] S_n^l[k] + I_{s_{\text{Part}d}}^l[k] + I_{b_{\text{All}d}}^l[k] + I_{\text{MAI}}^l[k] + n_d^l[k], \quad (22)$$

where we have

$$\begin{aligned} I_{s_{\text{Part}d}}^l[k] &= \sum_{i=1, \neq n}^N \sqrt{G_{s_i d}} h_{s_i d}^l[k] S_i^l[k] \gamma_{s_i s_n}, \\ I_{b_{\text{All}d}}^l[k] &= \sum_{e=1}^E \sqrt{G_{b_e d}} h_{b_e d}^l[k] P_{b_e}^l[k] \gamma_{b_e s_n}, \\ I_{\text{MAI}}^l[k] &= \sum_{w=1}^W \sqrt{G_{s_w d}} h_{s_w d}^l[k] S_w^l[k] \gamma_{s_w s_n}. \end{aligned} \quad (23)$$

The CCL between the PN sequences \mathbf{C}_i and \mathbf{C}_j is commonly represented by γ_{ij} , $i, j \in \{s_n, a_m, b_e, s_w\}$. We employ the Gold sequence set having a spreading factor of Q . Then, we specifically assign the PN sequences in order to guarantee that the CCL between any two nodes in the GANC aided SRAN constituted by the source group and the relay groups A as well as B is $-1/Q$. Let us define the transmit power of the SN s_n in a conventional single-link direct-transmission (DT) based DS-CDMA uplink as $\mathcal{P}_{s_n}^{\text{DT}}$. For the sake of a fair comparison, we assume that the overall transmit power of the system employing the proposed GANC aided SRAN and that of the system operating without a GANC aided SRAN are identical, which implies that

$$\sum_{n=1}^N \mathcal{P}_{s_n} + \sum_{e=1}^E \mathcal{P}_{b_e} = \sum_{n=1}^N \mathcal{P}_{s_n} + \sum_{m=1}^M \mathcal{P}_{a_m} = N \cdot \mathcal{P}_{s_n}^{\text{DT}}, \quad (24)$$

where \mathcal{P}_{s_n} , \mathcal{P}_{b_e} and \mathcal{P}_{a_m} represent the transmit powers of the SN s_n , the RN b_e and the RN a_m in the GANC aided SRAN, respectively. In this contribution, the system's equivalent SNR is defined as $\text{SNR} = 10 \log_{10} \left(\frac{\mathcal{P}_{s_n}^{\text{DT}}}{N_0} \right)$, where N_0 represents the receiver's noise. In the ensuing Section V, we will manage the transmit signal power of the SNs and RNs according to (24).

Furthermore, we also assume that the DS-CDMA based GANC aided SRAN benefits from perfect power control. Hence, as observed at the DN d of Fig. 5, all the received signals transmitted by the different users i.e. $\{s_n\}_{n=1}^N$ and $\{s_w\}_{w=1}^W$ should have the same signal power of \mathcal{P}_s . Based on our previous assumption of having perfect synchronisation within the GANC aided SRAN, the variances of the variables $I_{s_{\text{Part}d}}^l[k]$ and $I_{b_{\text{All}d}}^l[k]$ may be evaluated as

$$\text{Var} [I_{s_{\text{Part}d}}^l[k]] = (N-1) \frac{\mathcal{P}_s}{Q^2}; \quad \text{Var} [I_{b_{\text{All}d}}^l[k]] = \sum_{e=1}^E \frac{G_{b_e d} \mathcal{P}_{b_e}}{Q^2}. \quad (25)$$

However, it is challenging to maintain perfect synchronisation across the entire DS-CDMA system, especially when considering the UL of a high-load scenario. Hence we assume that the transmissions $\{s_w\}_{w=1}^W$ of the W interfering users are asynchronous with the transmissions $\{s_n\}_{n=1}^N$ of the N desired users. Then, based on the central limit theorem [24], the summation of W independent random variables may be modelled by the Gaussian distribution. Hence the component $I_{\text{MAI}}^l[k]$ in (22) may be approximated by a Gaussian variable. In line with [20], [27], by exploiting the Standard Gaussian Approximation method [28] derived by Pursley, the variance of the MAI in an asynchronous DS-CDMA system experiencing Rayleigh fading channels i.e. $I_{\text{MAI}}^l[k]$ may be approximated

by

$$\text{Var} [I_{\text{MAI}}^l] \approx \frac{1}{3Q} \sum_{w=1}^W (G_{s_w d} \mathcal{P}_{s_w}) = W \frac{\mathcal{P}_s}{3Q}. \quad (26)$$

As stated before, in order to detect the original information-bit streams $\{\mathbf{u}_n^l\}_{n=1}^N$, we also have to extract every symbol $P_{a_m}^{l+1}[k]$ from the received signal $\mathbf{y}_d^{l+1}[k]$ at the DN. Hence, similar to the operations invoked for generating $z_{s_n}^l[k]$ of (22), we match the chip-waveform matched-filter to the waveform of \mathbf{C}_{a_m} of the $(l+1)^{\text{st}}$ frame. Then, we input the received signal $\mathbf{y}_d^{l+1}[k]$ to the chip-matched filter. The associated output is given by

$$z_{a_m}^{l+1}[k] = \sqrt{G_{a_m d}} h_{a_m d}^{l+1}[k] P_{a_m}^{l+1}[k] + I_{a_{\text{Part}d}}^{l+1}[k] + I_{s_{\text{All}d}}^{l+1}[k] + I_{\text{MAI}}^{l+1}[k] + n_d^{l+1}[k], \quad (27)$$

where we have

$$\begin{aligned} I_{a_{\text{Part}d}}^{l+1}[k] &= \sum_{j=1, \neq m}^M \sqrt{G_{a_j d}} h_{a_j d}^{l+1}[k] P_{a_j}^{l+1}[k] \gamma_{a_j a_m}, \\ I_{s_{\text{All}d}}^{l+1}[k] &= \sum_{n=1}^N \sqrt{G_{s_n d}} h_{s_n d}^{l+1}[k] S_n^{l+1}[k] \gamma_{s_n a_m}, \\ I_{\text{MAI}}^{l+1}[k] &= \sum_{w=1}^W \sqrt{G_{s_w d}} h_{s_w d}^{l+1}[k] S_w^{l+1}[k] \gamma_{s_w a_m}. \end{aligned} \quad (28)$$

Similar to the derivations of (25) and (26), the variances of the interference components $I_{a_{\text{Part}d}}^{l+1}[k]$, $I_{s_{\text{All}d}}^{l+1}[k]$ and $I_{\text{MAI}}^{l+1}[k]$ in (27) may be evaluated as

$$\begin{aligned} \text{Var} [I_{a_{\text{Part}d}}^{l+1}] &= \sum_{j=1, \neq m}^M \frac{G_{a_j d} \mathcal{P}_{a_j}}{Q^2}, \quad \text{Var} [I_{s_{\text{All}d}}^{l+1}] = N \frac{\mathcal{P}_s}{Q^2}, \\ \text{Var} [I_{\text{MAI}}^{l+1}] &= W \frac{\mathcal{P}_s}{3Q}. \end{aligned} \quad (29)$$

According to (22) and (27), the estimates $\{z_{s_n}^l[k]\}_{n=1}^N$ of the information-bearing symbols $\{S_n^l[k]\}_{n=1}^N$ and the estimates $\{z_{a_m}^{l+1}[k]\}_{m=1}^M$ of the parity-bit bearing symbols $\{P_{a_m}^{l+1}[k]\}_{m=1}^M$ become available for the decoding of the cross-layer NC. Furthermore, according to the symmetry of the GANC aided SRAN, the despread signals $\{z_{s_n}^{l+1}[k]\}_{n=1}^N$ and $\{z_{b_e}^{l+2}[k]\}_{e=1}^E$ - which correspond to the information part and parity part of the cross-layer NC codeword - will be exploited by the cross-layer NC decoder for detecting the original information-bit streams⁷ $\{\mathbf{u}_n^{l+1}\}_{n=1}^N$. This process is similar to that specified by (20), (21), (22) and (27).

Furthermore, recall our arguments from Section II-C, namely that the PN sequences used by the RNs are readily available for our GANC aided SRAN, because they have already been assigned to the inactive users appointed as RNs. From this perspective, the average throughput \mathcal{T}_{ave} of the GANC aided SRAN is capable of approaching X bits/s, which represents the fact that in our GANC aided SRAN, the SNs are allowed to continuously broadcast their information-bit streams, namely during both the broadcast and cooperative phases. In order to visualize the throughput improvement achieved by our GANC aided SRAN, the average throughputs

⁷The information-bit streams $\{\mathbf{u}_n^{l+1}\}_{n=1}^N$ are broadcast in the $(l+1)^{\text{st}}$ frame and are represented by the dashed lines in the odd phase of Fig. 5.

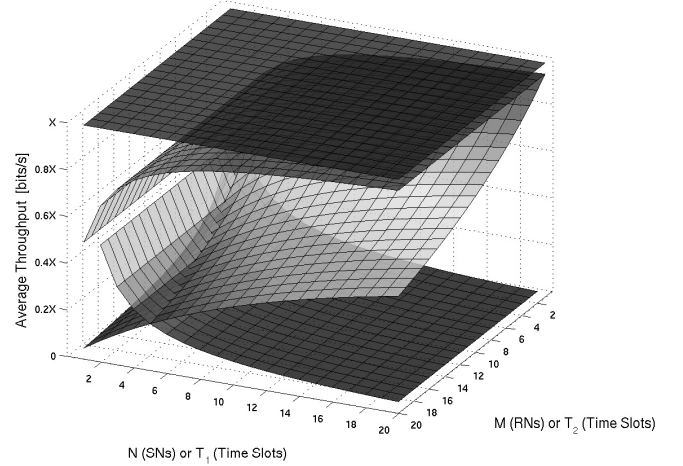


Fig. 6. The average throughput comparison among different network coding regimes.

of different network coding regimes are compared in Fig. 6, where all the benchmarks maintain the same diversity order for the sake of a fair comparison. In more detail, from the top to the bottom, the surfaces portrayed in Fig. 6 correspond to the average throughputs achieved by our GANC aided SRAN, by our GANC assisted basic cooperative network, by the GDNC regime of [14] and by the DNC regime of [10], respectively. Then, the relay groups A and B are independent of each other, which implies that the size of the relay group B and the channel code used as the cross-layer NC of relay group B can be different from that of relay group A. This indicates the convenient flexibility of the proposed GANC aided SRAN, again.

IV. NONCOHERENT ITERATIVE DETECTION BASED TRANSCEIVER DESIGN

Having introduced our GANC aided SRAN, we now need an appropriate practical transceiver. Since employing non-binary linear block codes as the cross-layer NC had also been discussed in the context of other network coding regimes [10], [13], [14], we would like to dedicate more attention to our RSC code based GANC regime both in this transceiver design section and in the ensuing simulation section. Hence we designed the noncoherent iterative detection aided architecture of Fig. 7. Without loss of generality, in Fig. 7, we assume that the size of the source group is $N = 3$. The relay groups A and B have the same size of $M = E = 2$ and employ the same cross-layer NC. Given the similarity of the information-bit streams $\{\mathbf{u}_n^l\}_{n=1}^N$ and $\{\mathbf{u}_n^{l+1}\}_{n=1}^N$ at the DN d , which were discussed in Section III⁸, we only discuss the detection of

⁸As indicated in Section III, $\{\mathbf{u}_n^l\}_{n=1}^N$ is broadcast during the l^{th} frame, which is related to the solid lines during the even phase of Fig. 5. We collect the despread signals $\{z_{s_n}^l\}_{n=1}^N$ and $\{z_{a_m}^{l+1}\}_{m=1}^M$ in order to implement cross-layer NC decoding at the DN d during the $(l+1)^{\text{st}}$ frame. Similarly, $\{\mathbf{u}_n^{l+1}\}_{n=1}^N$ is broadcast during the $(l+1)^{\text{st}}$ frame, which is related to the dashed lines in the odd phase of Fig. 5. We collect the despread signals $\{z_{s_n}^{l+1}\}_{n=1}^N$ and $\{z_{b_e}^{l+2}\}_{e=1}^E$ to detect $\{\mathbf{u}_n^{l+1}\}_{n=1}^N$ at the DN d during the $(l+2)^{\text{nd}}$ frame.

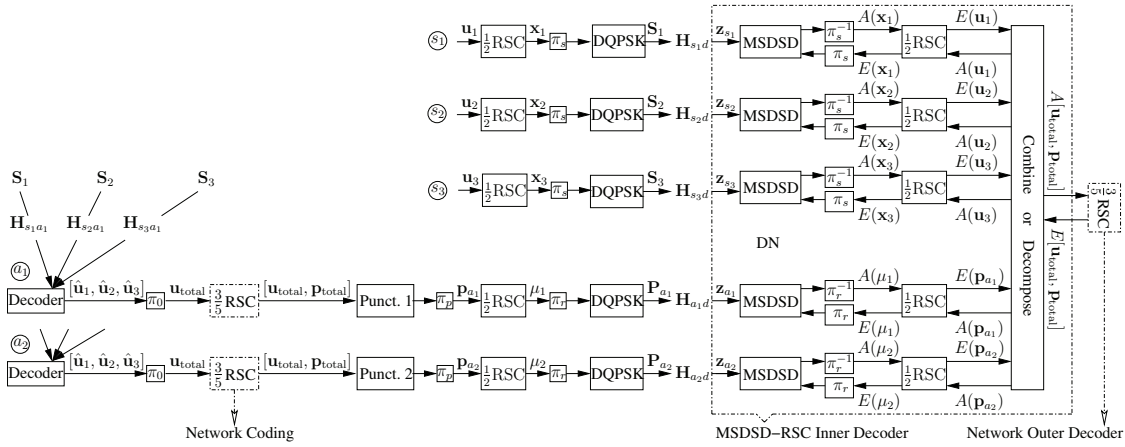


Fig. 7. The architecture of the noncoherent iterative detection assisted GANC aided SRAN.

$\{\mathbf{u}_n^l\}_{n=1}^N$ in Fig. 7. Furthermore, for simplicity, the superscript l is omitted from now on.

A. Source Node Architecture

In order to significantly enhance the error correction capability of the decoder, channel coding is invoked as an essential part of contemporary communication systems. Hence the classic RSC code having a coding rate of $R_{\text{code}} = \frac{1}{2}$ is employed at each SN s_n for encoding the original information-bit stream \mathbf{u}_n . In addition to the complex task of relaying, the RNs have to afford the power-hungry estimation of SR channels in support of coherent detection. Furthermore, the overhead of channel estimation also reduces the system's bandwidth efficiency. Hence, for the sake of obviating the extra energy and bandwidth consumption imposed by employing coherent detection, a differentially-encoded QPSK (DQPSK) modulator is amalgamated with a half-rate RSC channel encoder for generating the signal frame \mathbf{S}_n , which dispenses with pilot-based channel estimation⁹.

B. Relay Node Architecture

The SISO-MSDSD algorithm was devised by Pauli *et al.* [18] in support of soft-decision-aided iterative detection schemes in the context of noncoherent detection based communication systems. As a state-of-the-art noncoherent detection technique, it strikes an attractive trade-off between the BER performance attained and the complexity imposed. Hence the SISO-MSDSD scheme may be adopted as the first component decoder of the RN's receiver in Fig. 7. Then, in line with the SN's transmitter, the half-rate RSC decoder is adopted as the second component decoder of the RN's receiver. Consequently, a two-stage MSDSD-RSC decoder is created for detecting the information-bit streams $\{\mathbf{u}_n\}_{n=1}^N$ at each RN a_m , which is labelled as "Decoder" on the left of Fig. 7.

In the spirit of GANC, arbitrary channel codes can serve as the cross-layer NC. However, employing LDPC codes and

linear block codes for cross-layer NC was proposed in [13] and [14], respectively. In our low-complexity system, we opt for the conventional RSC code as our cross-layer NC and demonstrate that this low-complexity RSC code is capable of achieving a high performance. According to the first signal processing step stipulated in Section II-B, the coding rate of the cross-layer NC scheme should be $R_{\text{code}} = \frac{3}{5}$ at both a_1 and a_2 . As the second step, we concatenate a half-rate RSC code with a $\frac{5}{6}$ -rate puncturer, where the octally represented generator polynomials and the constraint lengths of the half-rate RSC code are (5, 7) and 3, respectively. As the third step, a_1 extracts half the bits from the entire set of parity-bits $\mathbf{p}_{\text{total}}$ as its parity-bit stream \mathbf{p}_{a_1} . Similarly, a_2 extracts the remaining parity-bits of $\mathbf{p}_{\text{total}}$ in order to create its parity-bit stream \mathbf{p}_{a_2} . Two punctures, namely "Punct.1" and "Punct.2" of Fig. 7 are employed for the appropriate partitioning of the bit stream $\mathbf{p}_{\text{total}}$. Furthermore, two interleavers, namely " π_0 " and " π_p " of Fig. 7 are employed for eliminating the potential fading-induced correlation, as stated in Section II-B.

The same transmitter may be employed at the RNs a_1 and a_2 as at the SN, in order to generate, as well as to modulate the parity-bit streams \mathbf{p}_{a_1} and \mathbf{p}_{a_2} for the sake of creating the transmitted signal frames of \mathbf{P}_{a_1} and \mathbf{P}_{a_2} , respectively.

C. Destination Node Architecture

For appropriately complementing the SN's and RN's transmitter architecture, five two-stage MSDSD-RSC decoders are employed at the DN, which were introduced in Section IV-B. They individually detect the information bit streams $\{\mathbf{u}_n\}_{n=1}^N$ and the parity-bit streams $\{\mathbf{p}_{a_m}\}_{m=1}^M$ based on both the despread signal frames $\{\mathbf{z}_{s_n}\}_{n=1}^N$ and $\{\mathbf{z}_{a_m}\}_{m=1}^M$ as well as on the information fed back by the cross-layer NC decoder of Fig. 7. The *extrinsic* information and *a priori* information, represented by $E(\cdot)$ and $A(\cdot)$ respectively, are interleaved and iteratively exchanged within the two-stage MSDSD-RSC decoder of Fig. 7 I_{inner}^d times.

As a benefit of the NC process implemented at the RNs, the parity-bit streams $\{\mathbf{p}_{a_m}\}_{m=1}^M$ carry redundant bits related to the information-bit streams $\{\mathbf{u}_n\}_{n=1}^N$. After appropriately rearranging the *extrinsic* information frames $\{E(\mathbf{u}_n)\}_{n=1}^N$ and $\{E(\mathbf{p}_{a_m})\}_{m=1}^M$, their combination, namely $A[\mathbf{u}_{\text{total}}, \mathbf{p}_{\text{total}}]$

⁹Although perfect channel-estimation (CE) aided coherent detection typically outperforms its noncoherent counterpart by about 3 dB, for a realistic practical CE, the difference becomes less substantial.

becomes capable of providing *a priori* information for the cross-layer NC decoder. Inspired by the JNCC scheme proposed by Hausl *et al.* in [15], we fed back the *extrinsic* information $E[\mathbf{u}_{\text{total}}, \mathbf{p}_{\text{total}}]$ provided by the cross-layer NC decoder to the five two-stage MSDSD-RSC decoders of Fig. 7. Naturally, the appropriate decomposition of $E[\mathbf{u}_{\text{total}}, \mathbf{p}_{\text{total}}]$ is required for mapping $E[\mathbf{u}_{\text{total}}, \mathbf{p}_{\text{total}}]$ to both $\{A(\mathbf{u}_n)\}_{n=1}^N$ and to $\{A(\mathbf{p}_{a_m})\}_{m=1}^M$. The five distributed two-stage MSDSD-RSC decoders actually constitute a single composite decoder conceived for cooperation with the cross-layer NC decoder of Fig. 7. Hence this architecture may be viewed as a three-stage MSDSD-RSC-NC receiver specifically created for the DN, where the composite decoder is constituted by five two-stage MSDSD-RSC decoder branches, acting in unison as the MSDSD-RSC inner decoder, while the cross-layer NC decoder acts as the outer decoder, as shown in Fig. 7.

Observe at the base station of [15, Fig 4] that there is no FEC decoder for specifically detecting the RN's parity-bits. Hence, after entering the output of the RD link “ \mathbf{y}_{43} ” into the “Network Dec.” of [15, Fig 4], the *extrinsic* information of the “Network Dec.” can only be fed back to those particular channel decoders, which are used for detecting the SN's information bits. This implies that the redundant information contained in the RD link is utilized only once. However, as a benefit of its reduced propagation distance, the RD link may achieve a higher integrity than the SD link. Hence the original JNCC scheme proposed in [15] only partially benefits from the iterations between the channel code and NC, as well as from the redundancy received via the RD link. Hence, if we directly apply the original JNCC scheme of [15] to our decoder at the DN of Fig. 5, it would be unable to exploit the *extrinsic* information $E[\mathbf{u}_{\text{total}}, \mathbf{p}_{\text{total}}]$ provided by the outer NC decoder for updating the *a priori* information $A(\mathbf{p}_{a_1})$ and $A(\mathbf{p}_{a_2})$ during the outer iterations between the MSDSD-RSC inner decoder and outer NC decoder. The resultant architecture may be referred to as a “partial-iteration” based three-stage MSDSD-RSC-NC decoder. By contrast, the proposed DN's receiver portrayed in Fig. 7 may be referred to as a “full-iteration” based three-stage MSDSD-RSC-NC decoder, where the *a priori* information $A(\mathbf{p}_{a_1})$ and $A(\mathbf{p}_{a_2})$ is updated during each outer iteration between the MSDSD-RSC inner decoder and outer NC decoder.

In order to visualize the discrepancy between the “partial-iteration” and “full-iteration” based three-stage MSDSD-RSC-NC decoders, the extrinsic information transfer (EXIT) [29] curves of their MSDSD-RSC inner decoders are compared in Fig. 8, where the sizes of the source group and relay group A were modified to $N = 2$ and $M = 2$, respectively¹⁰. It was shown in [30] that the area under the bit-based EXIT curve of the inner code approximates the maximum achievable coding rate of the outer channel code, while guaranteeing near-error-free communication. Hence the “full-iteration” based three-stage MSDSD-RSC-NC decoder always outperforms its “partial-iteration” based counterpart throughout the entire range of SNR values considered. In more detail, observe in Fig. 8 that as a detriment of losing the redundant information

¹⁰The purpose of opting for a different configuration with respect to that illustrated in Fig. 7 in this simulation is to demonstrate the discrepancy between the two schemes more explicitly.

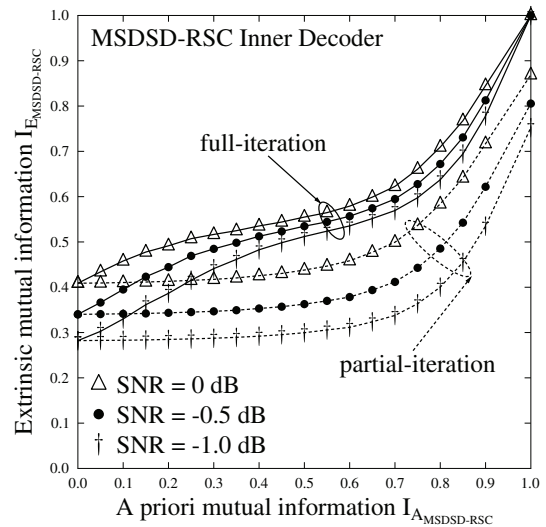


Fig. 8. EXIT curve comparison between the “partial-iteration” and “full-iteration” based three-stage MSDSD-RSC-NC decoders, where different SNR values are considered.

conveyed by the RD link, the EXIT curves associated with the “partial-iteration” based regime fails to approach the point of perfect convergence at (1, 1) in the EXIT chart, which implies that a BER floor is expected to emerge.

By observing the entire transceiver architecture of Fig. 7, again, we infer that when the size of the source group, or of the relay group A or B changes, we only have to modify the number of two-stage MSDSD-RSC decoder branches involved in the MSDSD-RSC inner decoder at the DN and then appropriately adjust the coding rate of the network code at the RNs and DN. The basic framework of the proposed transceiver still remains valid. Hence the proposed noncoherent “full-iteration” based three-stage transceiver also adapts to the time-variant network topologies.

V. SIMULATION RESULTS AND DISCUSSIONS

In our simulations, we assumed that the component SNs of the source group seen in Fig. 5 roam in each other's vicinity. Hence the distance between two SNs becomes negligible with respect to that between the SN and DN (or between the SN and RN). Accordingly, the entire source group is treated as a co-located unit, when considering the geometric relationship of the source group, relay group A, relay group B and DN. The same assumption is also applicable to the relay groups A and B. Hence the distances $D_{i,j}, i, j \in \{s_n, a_m, b_e, d\}$ are simplified to $D_{i,j}, i, j \in \{s, a, b, d\}$, where s, a, b, d represent the source group, relay group A, relay group B and DN, respectively. Moreover, we also assume having $M = E = 2$ and that an identical cross-layer NC is employed by the relay groups A and B. For the sake of concentrating our attention on the GANC aided SRAN, we assume having no interfering users i.e. $W = 0$. The main system parameters adopted in our simulations are summarized in Table I.

When two SNs constitute the source group of our GANC aided SRAN, the EXIT chart of the proposed three-stage MSDSD-RSC-NC decoder at the DN is seen in Fig. 9. Observe in Fig. 9 that an open tunnel exists between the EXIT curves

TABLE I
SYSTEM PARAMETERS

Channel Model	Time-Selective Rayleigh Fading Channel
Path-Loss Exponent	$\alpha = 3$
Normalized Doppler Frequency	$f_d = 0.01$
Destination Proportion	$D_{sa} : D_{sb} : D_{ad} : D_{bd} : D_{sd}$ $\approx 1 : 1 : 1 : 1 : 1.732$
PN Sequence	Gold sequence: $Q = 127$
Interfering Users	$W = 0$
Channel Coding	half-rate RSC
Cross-Layer NC	$\frac{N}{N+M}$ -rate RSC
Memory Length of RSC	$v = 3$
Modulation Scheme	DQPSK
MSDSD Observation Window Size	$N_{wind} = 6$
Inner Iterations of DN's Decoder	$I_{inner}^d = 2$
Size of Relay Group A (or B)	2

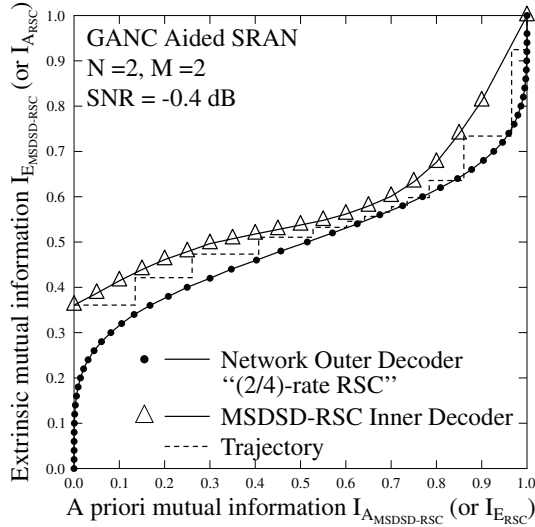


Fig. 9. The EXIT Chart of the DN's three-stage concatenated iterative decoder seen in Fig 7, where a $\frac{2}{4}$ -rate RSC code serves as the cross-layer NC. The remaining parameters are listed in Table I.

of the MSDSD-RSC inner decoder and the outer NC decoder of Fig. 7, when the system's overall equivalent SNR value reaches -0.4 dB. Furthermore, the associated Monte-Carlo simulation based decoding trajectory closely matches the EXIT curves and approaches the point of perfect convergence at $(1, 1)$ in the EXIT chart. Correspondingly, an infinitesimally low BER is expected beyond $\text{SNR} = -0.4$ dB. This is further evidenced in Fig.11, where the associated BER curve is seen to drop rapidly to an infinitesimally low value.

As stated in Section II-C, the ratio of the source group size to the relay group size impacts both the potential user-load reduction of the DS-CDMA system as well as the achievable reliability of our GANC aided SRAN. For the sake of investigating the effect of different source group size to relay group size ratios, we added one more SN to the source group. The associated EXIT chart performance of the proposed three-stage MSDSD-RSC-NC decoder recorded at the DN is shown in Fig. 10. This time, an open tunnel exists between the EXIT curves of the MSDSD-RSC inner decoder and the outer NC decoder for equivalent SNR values in excess of 2.2 dB. According to (7), this observation is in line with the basic philosophy that increasing the ratio of the source group size to the relay group size is equivalent to degrading the coding gain

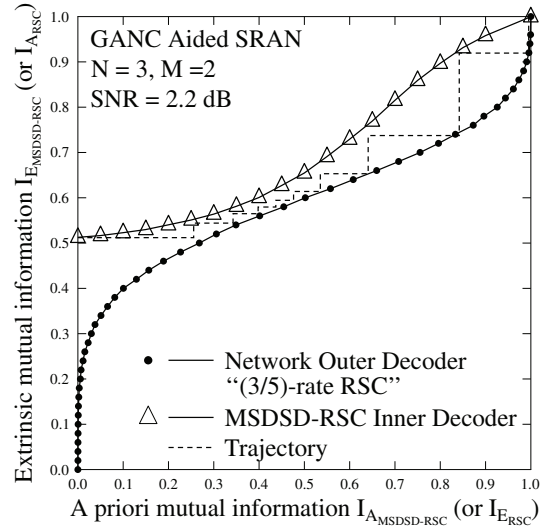


Fig. 10. The EXIT Chart of the DN's three-stage concatenated iterative decoder seen in Fig 7, where a $\frac{3}{5}$ -rate RSC code serves as the cross-layer NC. The remaining parameters are listed in Table I.

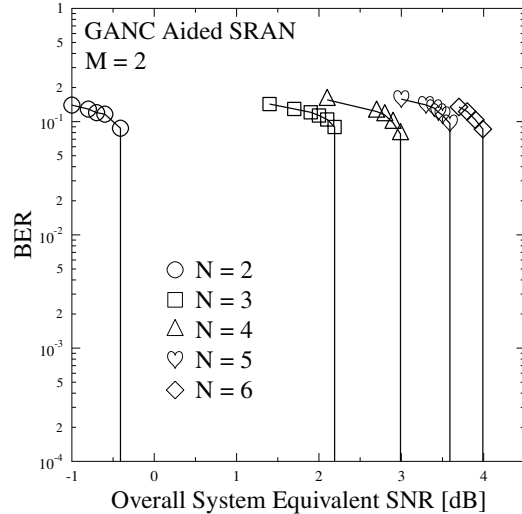


Fig. 11. The BER vs SNR performance when considering different network topologies.

of the cross-layer NC. Nevertheless, the benefit of this is that the potential user-load reduction imposed on the DS-CDMA system is mitigated.

In the spirit of our EXIT-chart analysis, the BER performance of different network topologies having different source group size to the relay group size ratios is provided in Fig. 11, where the source group size increased from $N = 2$ to $N = 6$, while the relay group size is fixed to $M = 2$. It is demonstrated in Fig. 11 again that increasing the source group size to relay group size ratio will degrade the system's BER performance. However, this degradation becomes more negligible, when increasing their ratio. As a benefit of employing the "full-iteration" based three-stage MSDSD-RSC-NC decoder of Fig. 7, a significant gain of about 10 dB is achieved compared to the simulation results shown in [15, Fig 9] at a target BER of 10^{-3} .

All the simulation results provided in this section are based on the assumption that a perfect detection is achieved at the RN. Firstly, this assumption is supported by our GANC scheme detailed in Section II-C, where the specific RN who cannot perfectly detect all the received SN's information-bit streams will be removed from the relay group. Secondly, as a benefit of the relay-aided path-loss reduction, as well as that of employing a two-stage MSDSD-RSC decoder at the RN, which has a powerful error-correction capability, the FER of the RN rapidly drops to a sufficiently low level. Consequently, we can successfully construct the GANC aided SRAN in the manner proposed in Section IV with a high probability of P_{success} . According to our investigation of the RN's detection¹¹, the system's equivalent SNR values, which are sufficiently high for reducing the system's BER to an infinitesimally low value for the cases of $N = \{3, 4, 5, 6\}$ as demonstrated in Fig. 11, are also capable of increasing P_{success} beyond 99.9%. This implies that for the $N = \{3, 4, 5, 6\}$ scenarios, the perfect detection condition expected at both the RN and at the DN can be simultaneously achieved for the SNR values observed in Fig. 11. In the case of $N = 2$, we have to increase the SNR value from -0.4 dB to 1.44 dB in order to simultaneously achieve perfect detection at both the RN and at the DN. Therefore the associated idealized simplifying assumption may not significantly impair the accuracy of our simulation results.

VI. CONCLUSIONS

In this contribution, we proposed a new GANC scheme. Upon intrinsically amalgamating the successive relaying protocol with our GANC aided cooperation, the GANC aided SRAN was created, where the typical 50% half-duplex relaying-induced throughput loss was converted to a potential user-load reduction of the DS-CDMA system. In order to improve the practicality of our investigations, a noncoherent iterative detection based transceiver was devised, which is capable of adapting to rapidly time-variant network topologies. The assumption of perfect detection at the RN will be eliminated in our future research by invoking the soft forwarding technique of [31] in our GANC aided cooperation.

REFERENCES

- [1] E. C. Van der Meulen, "Three-terminal communication channels," *Advanced Applied Probability*, vol. 3, pp. 120–154, 1971.
- [2] T. M. Cover and A. A. El Gamal, "Capacity theorems for the relay channel," *IEEE Trans. Inf. Theory*, vol. 25, pp. 572–584, Sep. 1979.
- [3] J. N. Laneman, N. C. Tse, and G. W. Wornell, "Cooperative diversity in wireless networks: efficient protocols and outage behavior," *IEEE Trans. Inf. Theory*, vol. 50, pp. 3062–3080, Dec. 2004.
- [4] R. Ahlswede, N. Cai, S.-Y. R. Li, and R. W. Yeung, "Network information flow," *IEEE Trans. Inf. Theory*, vol. 46, pp. 1204–1216, July 2000.
- [5] R. Koetter and M. Médard, "An algebraic approach to network coding," *IEEE/ACM Trans. Netw.*, vol. 11, pp. 782–795, Oct. 2003.
- [6] J. N. Laneman and G. W. Wornell, "Distributed space-time-coded protocols for exploiting cooperative diversity in wireless networks," *IEEE Trans. Inf. Theory*, vol. 49, pp. 2415–2425, Oct. 2003.
- [7] L. Xiao, T. Fuja, J. Kliewer, and D. Costello, "A network coding approach to cooperative diversity," *IEEE Trans. Inf. Theory*, vol. 53, pp. 3714–3722, Oct. 2007.

- [8] Z. Zhang, "Linear network error correction codes in packet networks," *IEEE Trans. Inf. Theory*, vol. 54, pp. 209–218, Jan. 2008.
- [9] M. Xiao and M. Skoglund, "M-user cooperative wireless communications based on nonbinary network codes," in *Proc. 2009 IEEE Inf. Theory Workshop*, pp. 316–320.
- [10] M. Xiao and M. Skoglund, "Multiple-user cooperative communications based on linear network coding," *IEEE Trans. Commun.*, vol. 58, pp. 3345–3351, Dec. 2010.
- [11] M. Xiao and T. Aulin, "Optimal decoding and performance analysis of a noisy channel network with network coding," *IEEE Trans. Commun.*, vol. 57, pp. 1402–1412, May 2009.
- [12] M. Xiao, M. Médard, and T. Aulin, "Cross-layer design of rateless random network codes for delay optimization," *IEEE Trans. Commun.*, vol. 59, pp. 3311–3322, Dec. 2011.
- [13] X. Bao and J. Li, "Adaptive network coded cooperation (ANCC) for wireless relay networks: matching code-on-graph with network-on-graph," *IEEE Trans. Wireless Commun.*, vol. 7, pp. 574–583, Feb 2008.
- [14] J. L. Rebelatto, B. F. Uchôa-Filho, Y. Li, and B. Vucetic, "Multiuser cooperative diversity through network coding based on classical coding theory," *IEEE Trans. Signal Process.*, vol. 60, pp. 916–926, Feb 2012.
- [15] C. Hausl and P. Dupraz, "Joint network-channel coding for the multiple-access relay channel," in *Proc. 2006 IEEE Commun. Society Sensor Ad Hoc Commun. Netw.*, pp. 817–822.
- [16] Y. Fan, C. Wang, J. Thompson, and H. V. Poor, "Recovering multiplexing loss through successive relaying using repetition coding," *IEEE Trans. Commun.*, vol. 6, pp. 4484–4493, Dec. 2007.
- [17] B. Rankov and A. Wittneben, "Spectral efficient protocols for half-duplex fading relay channels," *IEEE J. Sel. Areas Commun.*, vol. 25, pp. 379–389, Feb. 2007.
- [18] V. Pauli, L. Lampe, and R. Schober, "Turbo DPSK using soft multiple-symbol differential sphere decoding," *IEEE Trans. Inf. Theory*, vol. 52, pp. 1385–1398, Apr. 2006.
- [19] T. S. Rappaport, *Wireless Communications: Principles and Practice*. Prentice-Hall, 2002.
- [20] L. Hanzo, L.-L. Yang, E.-L. Kuan, and K. Yen, *Single and Multi-Carrier DS-CDMA : Multi-User Detection, Space-Time Spreading, Synchronisation and Standards*, 1st edition. John Wiley & Sons, 2005.
- [21] D. Tse and P. Viswanath, *Fundamentals of Wireless Communications*. Cambridge University Press, 2005.
- [22] J. W. Layland and R. J. McEliece, "An upper bound on the free distance of a tree code," Jet Propulsion Laboratory, California Institute of Technology, Pasadena, California, Space Programs Summary 37-62, vol. 3, pp. 63–64, Apr. 1970.
- [23] J. M. Jensen, "Bounds on the free distance of systematic convolutional codes," *IEEE Trans. Inf. Theory*, vol. 34, pp. 586–589, May 1988.
- [24] J. G. Proakis, *Digital Communications*, 5th edition. McGraw Hill, 2007.
- [25] C. Luo, Y. Gong, and F. Zheng, "Full interference cancellation for two-path relay cooperative networks," *IEEE Trans. Veh. Technol.*, vol. 60, pp. 343–347, Jan. 2011.
- [26] L. K. Kong, S. X. Ng, R. G. Maunder, and L. Hanzo, "Near-capacity cooperative space-time coding employing irregular design and successive relaying," *IEEE Trans. Commun.*, vol. 58, pp. 2232–2241, Aug. 2010.
- [27] J. Cheng and N. C. Beaulieu, "Accurate DS-CDMA bit-error probability calculation in Rayleigh fading," *IEEE Trans. Wireless Commun.*, vol. 1, pp. 3–15, Jan. 2002.
- [28] M. Pursley, "Performance evaluation for phase-coded SSMA communication—part I: system analysis," *IEEE Trans. Commun.*, vol. 25, pp. 795–799, Aug. 1977.
- [29] A. Ashikhmin, G. Kramer, and S. ten Brink, "Extrinsic information transfer functions: model and erasure channel properties," *IEEE Trans. Inf. Theory*, vol. 50, pp. 2657–2673, Nov. 2004.
- [30] I. Land, S. Huettinger, P. A. Hoeher, and J. B. Huber, "Bounds on information combining," *IEEE Trans. Inf. Theory*, vol. 51, pp. 612–619, Feb. 2005.
- [31] Y. Li, B. Vucetic, T. Wong, and M. Dohler, "Distributed turbo coding with soft information relaying in multihop relay networks," *IEEE J. Sel. Areas Commun.*, vol. 24, pp. 2040–2050, Nov. 2006.

¹¹For reasons of space economy, the FER performance of the RN and the derivation of the associated P_{success} value are not provided in this paper.



Li Li received the B.Eng. degree in information engineering from the University of Electronic Science and Technology of China (UESTC), Chengdu, China, in 2006 and the M.Sc. degree with distinction in wireless communications from the University of Southampton, Southampton, U.K., in 2009. He is currently working towards the Ph.D. degree in the Communications Group, School of Electronics and Computer Science, University of Southampton, Southampton, U.K., and participating in the European Union Concerto project. His research interests

include channel coding, iterative detection, non-coherent transmission technologies, cooperative communications, and network coding.



Li Wang (S'09-M'10) was born in Chengdu, China, in 1982. He received his B.Eng. degree in information engineering from Chengdu University of Technology (CDUT), Chengdu, China, in 2005 and his M.Sc. degree with distinction in radio frequency communication systems from the University of Southampton, UK, in 2006. Between October 2006 and January 2010, he was pursuing his Ph.D. degree in the Communications Group, School of Electronics and Computer Science, University of Southampton, while he also participated in the Delivery Efficiency

Core Research Programme of the Virtual Centre of Excellence in Mobile and Personal Communications (Mobile VCE). Upon completion of his Ph.D. in January 2010, he conducted research as a Senior Research Fellow in the School of Electronics and Computer Science at the University of Southampton. During this period, he was involved in Project #7 of the Indian-UK Advanced Technology Centre (IU-ATC): Advanced air interface technique for MIMO-OFDM and cooperative communications. In March 2012, he joined the R&D center of Huawei Technologies in Stockholm, Sweden, working as a Senior Engineer of Baseband Algorithm Architecture. He has published over 30 research papers in IEEE/IET journals and conferences, and he also co-authored one John Wiley/IEEE Press book. He has broad research interests in the field of wireless communications, including PHY layer modeling, link adaptation, cross-layer system design, multi-carrier transmission, MIMO techniques, CoMP, channel coding, multi-user detection, non-coherent transmission techniques, advanced iterative receiver design, and adaptive filter.



Lajos Hanzo FEng, FIEEE, FIET, Fellow of EURASIP, D.Sc. received his degree in electronics in 1976 and his doctorate in 1983. In 2009 he was awarded the honorary doctorate "Doctor Honoris Causa" by the Technical University of Budapest. During his 35-year career in telecommunications he has held various research and academic posts in Hungary, Germany, and the UK. Since 1986, he has been with the School of Electronics and Computer Science, University of Southampton, UK, where he holds the chair in telecommunications. He has

successfully supervised 80 Ph.D. students, co-authored 20 John Wiley/IEEE Press books on mobile radio communications totalling in excess of 10 000 pages, published 1300 research entries at IEEE Xplore, acted both as TPC and General Chair of IEEE conferences, presented keynote lectures, and has been awarded a number of distinctions. Currently, he is directing a 100-strong academic research team, working on a range of research projects in the field of wireless multimedia communications sponsored by industry, the Engineering and Physical Sciences Research Council (EPSRC) UK, the European IST Programme, and the Mobile Virtual Centre of Excellence (VCE), UK. He is an enthusiastic supporter of industry and an academic liaison and he offers a range of industrial courses. He is also a Governor of the IEEE VTS. During 2008–2012, he was the Editor-in-Chief of the IEEE Press and a Chaired Professor at Tsinghua University, Beijing. His research is funded by the European Research Council's Senior Research Fellow Grant. For further information on research in progress and associated publications, please refer to <http://www-mobile.ecs.soton.ac.uk> or <http://www-mobile.ecs.soton.ac.uk>.